Published in final edited form as:
J Immunol. 2009 April 1; 182(7): 4093–4106. doi:10.4049/jimmunol.0803317.

PTPN22 deficiency cooperates with the CD45 E613R allele to break tolerance on a non-autoimmune background

Julie Zikherman[1], **Michelle Hermiston**[2], **David Steiner**[3], **Kiminori Hasegawa**[4], **Andrew Chan**[4], and **Arthur Weiss**[5]

[1]Division of Rheumatology, Rosalind Russell Medical Research Center for Arthritis, Department of Medicine, UCSF, San Francisco, CA

[2]Department of Pediatrics, UCSF, San Francisco, CA

[3]Medical Scientist Training Program, UCSF, San Francisco, CA

[4]Department of Immunology, Genentech, Inc., South San Francisco, CA

[5]Division of Rheumatology, Rosalind Russell Medical Research Center for Arthritis, Department of Medicine, Howard Hughes Medical Institute, UCSF, San Francisco, CA

Abstract

Pep and CD45 are tyrosine phosphatases whose targets include the Src-family kinases, critical mediators of antigen receptor signaling. A polymorphism in *PTPN22*, the gene that encodes the human Pep ortholog Lyp, confers susceptibility to multiple human autoimmune diseases in the context of complex genetic backgrounds. However, the functional significance of the R620W risk allele is not clear. We report that misexpression of wild type or R620W Pep/Lyp in Jurkat cells, in the context of its binding partner Csk, unmasks the risk allele as a hypomorph.

It has been shown previously that, although Pep deficient mice on the B6 background have hyper-responsive memory T cells, autoimmunity does not develop. Mice containing a point mutation in the CD45 juxtamembrane wedge domain (E613R) develop a B cell-driven lupus-like disease on the mixed 129/B6 background, but not on the B6 background. We studied the ability of Pep deficiency to act as a genetic modifier of the CD45 E613R mutation on the non-autoimmune B6 background in order to understand how complex susceptibility loci might interact in autoimmunity. Here we report that double mutant mice develop a lupus-like disease as well as lymphadenopathy, polyclonal lymphocyte activation, and accelerated memory T cell formation. Following antigen receptor stimulation, peripheral B cells in the double mutant mice phenocopy hyper-responsive CD45 E613R B cells, whereas peripheral T cells respond like $Pep^{-/-}$ T cells. These studies suggest that $Pep^{-/-}$ T cells in the context of a susceptible microenvironment can drive hyper-responsive CD45 E613R B cells to break tolerance.

Keywords

phosphatase; autoimmunity; lupus; tyrosine phosphorylation

Corresponding Author : Arthur Weiss; aweiss@medicine.ucsf.edu Department of Medicine, Division of Rheumatology Department of Microbiology and Immunology 513 Parnassus, Room S-1032C, Box 0795 San Francisco, CA 94143-0795 (415) 476-8983 tel (415) 502-5081 fax.

Introduction

Human autoimmune diseases arise from environmental challenge in the context of cooperating susceptibility loci, each of which independently confers a small relative risk. Modeling and understanding the mechanisms that underlie such interactions in a tractable genetic system such as the mouse has been challenging.

A polymorphism in the human gene *PTPN22* (C1858T / R620W) confers risk for developing multiple autoimmune diseases including rheumatoid arthritis (RA), systemic lupus erythematosus (SLE) and type 1 diabetes (1–3). Indeed, *PTPN22* R620W was the second most significant risk allele identified in two unbiased whole genome scans for rheumatoid arthritis, although the odds ratio associated with carrying the risk allele is quite modest, with a value of less than two (4–6). Nevertheless, human autoimmune disease has a striking genetic contribution; RA heritability has been estimated at 60% (7). Clearly even potent susceptibility loci must interact with one another to account for this phenomenon. How then can this complex process be effectively modeled and studied?

PTPN22 encodes Lyp, a hematopoietic phosphatase the mouse homolog of which is Pep (PEST-domain enriched tyrosine phosphatase) (8,9). Pep/Lyp negatively regulates TCR signaling by dephosphorylating the activating tyrosine of the Src-family kinase (SFK) Lck (10,11). SFKs are critical mediators of signal transduction by ITAM-bearing immunoreceptors such as the TCR (12).

Pep is cytoplasmic but is brought into proximity of its target, coreceptor-associated Lck, at the plasma membrane via its constitutive association with the cytoplasmic tyrosine kinase Csk (10,13). Csk phosphorylates the inhibitory tyrosine of the SFKs and is itself a potent negative regulator of TCR signaling (14). Csk is recruited to the membrane by the transmembrane adaptor PAG, which is phosphorylated under basal conditions (15,16). Following TCR ligation, PAG is rapidly dephosphorylated, releasing Csk from the membrane (16). Pep and Csk interact functionally as well as physically to cooperatively inhibit TCR signaling (10, 11). This cooperative inhibition has been shown to depend upon the C-terminal proline rich sequence (PRS) of Pep and the SH3 domain of Csk (10). The PRS of Pep (613–621 PPPLPE***R***T), containing the critical R620 residue, is absolutely required for this association and for cooperative inhibition of TCR signaling (13).

To complement in vitro over-expression studies, Pep-deficient ($Pep^{-/-}$) mice provide in vivo support for a negative regulatory role in TCR signaling (17). The phenotype is however surprisingly subtle; TCR signaling is enhanced at the CD4+CD8+ (double positive) stage of thymocyte development and in the effector/memory compartment of peripheral T cells, but naïve T cells and B cells appear to have no functional abnormality. While $Pep^{-/-}$ mice develop an expanded effector/memory T cell compartment and increased numbers of spontaneous germinal centers, no autoantibodies or frank autoimmune disease are observed on the B6 genetic background. One possible explanation for this subtle phenotype is redundancy with the ubiquitously expressed, related phosphatase PTP-PEST (18).

The R620W polymorphism partially disrupts the association of Pep/Lyp with Csk (1,19). These data are consistent with a critical role for the PRS domain, and suggest that the R620W allele might represent a hypomorphic variant. However, evidence from genetic studies does not clearly identify either a pure recessive or dominant effect of the polymorphism in RA (HET odds ratio 1.98, HOM odds ratio 3.32) (4). Relatively few in vitro functional studies of the polymorphism have been reported. In a Jurkat overexpression study, the R620W allele of Lyp exerted more potent inhibition of TCR signaling than wild type (19). Importantly, the polymorphism was not studied in the context of its binding partner Csk to identify its effect on synergistic inhibition of TCR signaling. More recently, another group has studied the

functional consequences of the R620W variant directly in primary human T cells from heterozygous and homozygous carriers of the polymorphism. These studies found impaired calcium flux and upregulation of activation markers in response to TCR ligation in peripheral blood memory T and B cells. Notably, naïve T cell function was normal and no significant differences in IL-2 production or proliferation were detectable (20). Three additional studies in which primary PBMCs from patients with type I diabetes or myasthenia gravis who carry the R620W allele have been subjected to functional assays report mixed results (19,21,22).

The functional consequences of the R620W polymorphism, the mechanism by which *PTPN22* acts as an autoimmune susceptibility locus, and the genetic contexts in which this might occur remain unclear. Given the significance of *PTPN22* for human autoimmunity, we sought to establish systems in which we could model and study the risk allele *in vitro* in the context of Csk and *in vivo* in the context of a permissive genetic background. To this end, we studied co-expression of Csk and Pep as well as Lyp variants in Jurkat cells. To model the genetic cooperation of *PTPN22* with other autoimmune susceptibility loci, we took advantage of CD45 E613R mice in which hyper-responsive B cells, characteristic of human and murine SLE, drive a lupus-like disease only on certain genetic backgrounds.

CD45 is a receptor-like tyrosine phosphatase expressed at high levels on all nucleated hematopoietic cells (23). CD45 deficiency in humans and mice leads to SCID phenotypes, revealing a crucial positive role for CD45 in immunoreceptor signaling and lymphocyte development (24–27). Polymorphisms in CD45 which influence regulated splicing are associated with autoimmune disease in humans (28). CD45 dephosphorylates the negative regulatory tyrosine of SFKs, thereby “priming” cells to respond to signals through immunoreceptors (23). This positive regulatory role is normally counterbalanced by the cooperating module of Csk/Pep.

Our lab previously identified a critical membrane proximal residue (E613) in the cytoplasmic domain of CD45 which mediates dimerization-induced inhibition of phosphatase activity. Mutation of this site to an arginine ablates such inhibition (29,30). Further support for the critical regulatory role of this residue was provided by the E613R `Wedge' ($CD45^{W/W}$) knockin mouse which developed lymphoproliferation, polyclonal lymphocyte activation, autoantibodies, and immune complex glomerulonephritis, a phenotype reminiscent of human SLE (31). Genetic deletion of B cells revealed that the lymphoproliferation was B cell driven (32). At the cellular level, B cells were extremely hyper-responsive to B cell receptor signaling, a characteristic shared with spontaneous and engineered mouse models of lupus as well as B cells from patients with SLE (32–35).

However, further backcrossing of the original knockin revealed a remarkable background dependence of the disease phenotype (Hermiston et al., manuscript in preparation). B cell hyper-responsiveness was noted on all backgrounds, but the original disease phenotype was recapitulated only on the B6/129 F1 background. Indeed, CD45 E613R mice on the pure B6 background develop no autoantibodies or end-organ disease. Therefore, CD45 E613R effectively functions as a murine autoimmune susceptibility allele in which “lupus-like” B cells cooperate with other factors. This result suggested that the $CD45^{W/W}$ B6 mouse might provide a suitable background against which to study candidate genetic modifiers such as *PTPN22*.

Here we report that misexpression of wild type and R620W Pep and Lyp alleles in the context of Csk in Jurkat cells unmasks R620W as a hypomorphic allele. We took advantage of Pep-deficient mice as a model of the hypomorphic human risk allele, albeit a more extreme allele. We crossed the $Pep^{-/-}$ mice onto the non-autoimmune $CD45^{W/W}$ B6 background in order to model how subtle susceptibility loci might cooperate in human autoimmune disease. We found that these alleles cooperate to break tolerance on the non-autoimmune B6 genetic background.

Indeed, double mutant $CD45^{W/W}/Pep^{-/-}$ mice develop lymphadenopathy and splenomegaly, autoantibodies, glomerulonephritis and premature mortality. The cellular phenotype is characterized by polyclonal B and T cell activation as well as early and progressive expansion of the memory T cell compartment. Studies of antigen receptor signal transduction revealed that peripheral B cells in double mutant mice respond like single mutant $CD45^{W/W}$ B cells while peripheral T cells resemble single mutant $Pep^{-/-}$ T cells. In contrast, thymic signaling reflects cooperation between the two mutant alleles. These studies suggest that $Pep^{-/-}$ T cells in the context of a susceptible microenvironment drive $CD45^{W/W}$ B cells to break tolerance.

Materials and Methods

Mice

CD45 E613R ($CD45^{W/W}$) mice were generated as previously described (31). All experiments described in this manuscript involve mice backcrossed at least 9 generations onto the B6 background. $Pep^{-/-}$ mice (17) were originally generated on a pure B6 background and were obtained from A. Chan (Genentech). $Dnase1^{-/-}$ mice (37) were backcrossed for at least 9 generations onto B6 background and were obtained from T. Moroy. All animals were genotyped by PCR. Mice were used at 6–10 weeks of age for all functional and biochemical experiments. Mice used at older ages for phenotypic assessment are indicated in the manuscript. All animals were housed in a specific pathogen free facility at UCSF according to University and National Institutes of Health (NIH) guidelines.

Histology

Tissues were fixed in 10% buffered formalin for a minimum of 24 hours and were subsequently embedded in paraffin, sectioned, and stained using standard techniques. Sections were then subjected to hematoxylin and eosin staining.

Serum processing and ELISA

Serum was prepared from blood harvested either by cardiac puncture at the time of sacrifice or via tail bleed with the use of serum separator tubes (BD microtainer). Serum immunoglobulin levels were determined by enzyme-linked immunosorbent assay (ELISA) using an immunoglobulin isotyping kit and standards (Southern Biotech) as per the manufacturer's protocol. IgG antibodies to dsDNA in sera from individual mice were measured by ELISA as described (54). The results were expressed in arbitrary ELISA units relative to a standard positive sample derived from MRL/lpr mice.

ANA Immunofluorescence staining

Hep2A cell 12-well slides (iNOVA) were stained with mouse serum prepared as above at 1:100 dilution. Slides were incubated with serum for 30 minutes, washed, and incubated with FITC-conjugated goat anti-mouse IgG (Jackson Immunochemicals) for 10 minutes, washed, coverslipped, and then visualized using a Zeiss microscope. MRL/lpr sera was used as a positive control and B6 serum was used as a negative control.

Antibodies and Reagents

Antibodies to murine CD1d, CD3, CD4, CD5, CD8, CD11b, CD19. CD21, CD23, CD44, CD62L, CD69, CD138, AA4.1, Gr-1, IgD, IgM, or B220 conjugated to FITC, PE-Texas Red, PE, PerCP-Cy5.5, PE-Cy5.5, PE-Cy7, Pacific Blue, APC, or Alexa 647 were obtained from eBiosciences or BD Biosciences. Antibodies to intracellular IFNγ, IL-17, IL-10, and IL-4 conjugated to PE or APC were obtained from BD Biosciences. Erk1 and 2 antibodies were obtained from Santa Cruz. Myc (9B11) and Phospho-Erk antibodies used for western blotting and flow cytometry were obtained from Cell Signaling. Polyclonal antibodies to Pep (PEP1

and PEP2 generated against PRS1 and 2 domains respsectively) were compliments of A. Chan (Genentech). Csk antibody (C-20 clone) was obtained from Santa Cruz. Stimulatory anti-CD3ε anti-Armenian hamster antibodies (2C11 clone) were obtained from Harlan. Goat anti-armenian hamster IgG(H+L) antibodies, goat anti-mouse IgM $(Fab')_2$, and goat anti-rabbit IgG antibodies conjugated to either PE or APC were obtained from Jackson Immunoresearch.

Flow Cytometry

Single cell suspensions were prepared from lymph node, spleen, and thymus. Fc receptors were blocked with rat anti-CD16/32 (2.4G2, BD Biosciences). 10^6 cells were stained with indicated antibodies and analyzed on FACSCalibur (Becton Dickson) or CyAN ADP (DAKO). Forward and side scatter exclusion was used to identify live cells. Data analysis was performed using FlowJo (v8.5.2) software (Treestar Incorporated, Ashland, OR).

Lymphocyte stimulation

Single cell suspensions were prepared from lymph node, spleen, and thymus. For soluble stimulation (whole cell lysates and flow cytometric analysis of calcium flux or Erk phosphorylation), T cells were stimulated at 37°C in suspension with anti-CD3ε followed after 30s by cross-linking with goat anti-armenian hamster IgG. Plate-bound stimulation of T cells (for activation marker upregulation) was carried out by precoating 96 well plates with anti-CD3ε and incubating plates overnight at 4°C. Cells were then plated at a concentration of 2×10^6/ml and harvested after 15 h incubation at 37°C. B cell stimulation, whether soluble or plate bound was carried out with soluble goat anti-mouse IgM $(Fab')_2$.

Calcium Flux

Single cell suspensions of thymocytes or lymphocytes were loaded with 4μg /10^7 cells of Fluo4-AM (Molecular Probes) for 30 minutes at 37°C in complete culture media. T cells were stimulated (as described above) and collected at 37°C on a FACSCalibur. Intracellular calcium concentration was determined using the FlowJo kinetic function. Double positive thymocytes were gated using a small size gate (>95% purity), while peripheral T cells were gated using dump staining for B cells and either CD8 or CD4. Cells were stimulated with ionomycin for positive control.

Intracellular staining for phospho-Erk

Thymocytes, spleen, or lymph node cells were harvested into serum-free media. Single cell suspensions were rested at 37°C for at least 30 minutes prior to stimulation (as described above) and subsequently fixed to terminate stimulation. Cells were permeablized using 95% ice-cold methanol (EMS) for 30 min, stained with phospho–Erk antibody for 1 h, stained with surface markers and donkey anti–rabbit–PE or APC for 1 h, and fixed. Data were collected on a FACSCalibur and analyzed using FlowJo software.

Intracellular staining for Pep

Single cell suspensions from spleen or LN were resuspended in FACS buffer. Cells were then surface stained, fixed, stained for intracellular Pep with PEP1 or PEP2 polyclonal antibodies (described above) in saponin-based medium B (Caltag), washed with Perm/Wash (BD Biosciences), followed by secondary staining with Goat-anti-rabbit antibody (Jackson Immunoresearch) conjugated to PE. Data were collected on a FACSCalibur and analyzed using FlowJo software.

T cell purification

B cells, CD4 T cells or CD8 T cells were purified with MACS columns (Miltenyi) as per manufacturers protocol and subsequently used for whole cell lysates.

Immunoblotting

Whole cell lysates were generated by lysing stimulated or unstimulated cells in SDS sample buffer. Samples were analyzed by SDS-PAGE and immunoblotting. Blots were visualized with Western Lightning ECL reagent (PerkinElmer Life Sciences, Inc.) and a Kodak Imaging Station.

Expression vectors—Murine Pep construct in pCMV expression vector was obtained from MGC library via Invitrogen. Lyp1 C1858*R620 allele was cloned from a Jurkat cDNA library. Site directed mutagenesis using QuikChange (Stratagene) was performed to introduce the R619W (murine homolog) /R620W residue change into Pep and Lyp1 respectively. Both alleles were then subcloned into a pEF expression vector (Invitrogen). Myc-tagged murine Csk in the pEF expression vector were obtained from Jaime Schoenborn (Weiss lab).

Jurkat experiments—Jurkat cells were grown in RPMI supplemented with 10% FCS at density $0.1 - 0.6 \times 10^6$ cells / ml without supplementary antibiotics. Constructs with Csk, wild type Pep, R619W Pep, wild type Lyp1, R620W Lyp1, hCD16, and /or GFP under the control of pEF promoter were transiently transfected via electroporation. A total of 20ug of plasmid was introduced into 12×10^6 cells /condition. Empty vector was included to maintain constant plasmid concentration. Functional studies were performed and lysates were generated 12–15 hours after transfection. Lysates were made with 1% NP40 lysis buffer. Csk, Lyp and Pep expression levels were probed by western blot with Myc, Csk, and Pep antibodies (described above). For functional studies of Erk phosphorylation, cells were rested in serum free RPMI at 37°C for at least 15 minutes prior to stimulation with C305 or PMA for 2 minutes. Cells were then immediately fixed and subjected to permeabilization and staining for phospho-Erk as described above for primary cells. For analysis of calcium flux, cells were loaded with Fluo3 and Fura Red (Mol Probes) for 30 minutes at 37°C, surface stained for the transfection marker hCD16 (BD), stimulated with C305 and collected at 37°C on a FACSCalibur. Intracellular calcium concentration was determined using the FlowJo kinetic function and Fluo3/FuraRed ratio.

Results

Pep is expressed predominantly in T cells

The ubiquitous expression of CD45 on all nucleated hematopoietic cells is well-established (23). Pep/Lyp expression is not as well-characerized. Lyp message has been detected in human thymus and peripheral lymphoid tissue, including B and T cells (8). Lyp protein expression has been seen in thymocytes and primary human T cells (8). In order to identify which immune cell subsets might contribute to autoimmune disease in mice and which cellular context would serve best to study the functional consequences of the risk allele, we defined the protein expression pattern of Pep in mice. Due to the presence of non-specific bands, we controlled for antibody specificity by using Pep-deficient cell lysates. Using a combination of western blotting (Figure 1A) and flow cytometric detection of intracellular staining (Figure 1B) with two independent polyclonal antibodies to Pep, we found that Pep is expressed at appreciable levels predominantly in T cells. We detected expression in thymocyte subsets as well as peripheral T cells and noted that CD8 T cells express considerably more Pep than CD4 T cells (Figure 1A and data not shown). We also noted increased expression in $CD69^{hi}$ activated and $CD44^{hi}$ memory/effector T cells, but were unable to detect significant protein expression in myeloid subsets, B cells, whole spleen or bone marrow (Figure 1 and data not shown). This is

consistent with reports that Lyp is upregulated in T cells upon TCR stimulation, and absence of detectable Lyp message in human bone marrow or myeloid cell lines (8). This result is furthermore consistent with the absence of a B cell phenotype in the $Pep^{-/-}$ mice (17).

The R620W allele of PTPN22 is a hypomorph in the context of Csk

In order to clarify the functional consequences of the human R620W *PTPN22* polymorphism, we undertook in vitro studies of the risk allele in the Jurkat human T cell line. The Jurkat cell line is an appealing model system in which to pursue these studies because it has been recently shown that PTP-PEST, a Pep-related phosphatase with partially redundant functions, is not expressed in Jurkat cells (and downregulated in primary effector T cells) (18). This context supplies an opportunity to unmask Pep-dependent events.

Overexpression of phosphatases is difficult to evaluate because of the promiscuity of their target selection. Both mislocalization and stoichiometric perturbations of overexpression can lead to `ectopic' dephosphorylation within the cell and off-target effects which are not physiologic. It has been shown that under basal conditions, 25–50% of Pep in the cell is bound to Csk (13). Because Csk targets Pep to its substrate Lck by virtue of the interaction between the Csk SH3 domain and the Pep PRS domain which contains the R620 residue, it is critical to study the R620W allele in the context of Csk. We studied Pep R620W in the context of cooperating Csk in order to reduce over-expression and to limit off-target effects which may have confounded earlier studies. We used flow cytometric readouts of Erk phosphorylation to permit cell-specific assessment of a wide range of construct expression levels in order to carefully control for overexpression and dose.

In co-transfection studies in the Jurkat cell line with Pep and Csk vectors, we have been able to show that Csk and wild type (WT) Pep can cooperate synergistically to inhibit Erk phosphorylation following TCR stimulation (Figure 2). In these experiments we consistently found that wild type Pep inhibits Erk phosphorylation more potently than the R620W allele, both independently and more so in the context of Csk (Figure 2). Furthermore, this functional readout correlates with co-transfected GFP levels in a flow-based assay (Figure 2B). Relative function of the WT and R620W Pep alleles is qualitatively unchanged at both high and low GFP levels in our studies (Figure 2B and data not shown), suggesting overexpression artifact does not play a role here.

Total transfection efficiency was comparable between samples (data not shown) and Pep as well as Csk protein levels were comparable between samples (Figure 2A). By using murine Pep in our studies, we were able to take advantage of a polyclonal antibody to murine Pep that does not recognize endogenous human Lyp in order to identify total levels of misexpressed protein. By using myc-tagged murine Csk which migrates more slowly than endogenous untagged Csk, we could distinguish the two by western. We can identify very modest levels of overexpression and make use of endogenous Csk levels as an accurate loading control (Figure 2A).

Human Lyp and murine Pep proteins are only about 70% conserved, although the critical PRS1 domain which mediates Csk association is completely conserved (8). We therefore performed parallel experiments in Jurkat cells using myc-tagged Lyp1 C1858*R620 and T1858*W620 alleles. We observed similar effects of Lyp and Pep homologs on inhibition of TCR-induced Erk phosphorylation (Figure 3 A–C). The human Lyp1 C1858*R620 wild type allele more potently inhibits TCR signaling than the T1858*W620 risk allele, both independently and in the context of Csk. As in Pep misexpression experiments, transfection efficiency and dose was controlled for by GFP co-transfection as well as western blot detetction of Myc-tagged Lyp and Csk (Figure 3A,B). Furthermore, in both Pep and Lyp experiments, no defect in PMA-

induced Erk phosphorylation was observed, implying a proximal target for Pep/Lyp function in TCR signaling (Figure 2B, 3B).

In order to assess a distinct functional readout, we assayed the effect of Lyp/Csk co-expression upon TCR-induced calcium flux by flow cytometry. By gating on the co-transfected surface marker CD16, we observed relatively stronger inhibition of calcium entry by the Lyp1 C1858*R620 wild type allele than by the T1858*W620 risk allele in the context of Csk (Figure 3D). This effect was dose-dependent as assessed by CD16 gating (data not shown). Because calcium and Erk signals are similarly perturbed by Lyp/Csk misexpression, we conclude that Lyp and Csk must cooperatively inhibit TCR signaling at or proximal to the Lat/Slp76 signalosome at which these signals diverge. This is consistent with known and putative Lyp substrates, including Lck, Zap70, CD3ε, ζ and Vav (36). These flow-based readouts effectively capture the functional phenotype of the Pep and Lyp phosphatases. More proximal substrates such as Lck 394 are difficult to perturb and assay in the context of minimal misexpression.

From these studies, we conclude that the R620W human risk allele of *PTPN22* functions as a hypomorph in the context of TCR signal transduction, and may be appropriately modeled using the Pep-deficient mouse.

Double mutant $CD45^{W/W}/Pep^{-/-}$ mice develop a lupus-like disease

CD45 E613R ($CD45^{W/W}$) mice, previously backcrossed for more than 9 generations to the B6 background, were crossed to $Pep^{-/-}$ mice, originally generated on a B6 background. Double mutant $CD45^{W/W}/Pep^{-/-}$ B6 mice homozygous for each of the two mutant alleles were generated and aged. In a parallel experiment, $Dnase1^{-/-}$ mice were crossed onto the B6 $CD45^{W/W}$ background and aged ($CD45^{W/W}/Dnase1^{-/-}$). Dnase1 has also been shown to be a murine lupus susceptibility locus, but is also not associated with autoantibodies on the B6 background (37).

The $CD45^{W/W}/Pep^{-/-}$ mice developed IgG autoantibodies to double stranded DNA in a partially penetrant fashion, with elevated titers detectable by ELISA as early as 3 months of age and increasing with time (Figure 4A). Titers in some mice reached levels comparable to those seen in the MRL/lpr lupus prone mouse model (arbitrary ELISA units = 1000) by 9 months of age (Figure 4A and B). Autoantibody specificity was also assayed by indirect immunofluorescence staining of Hep2A cells and revealed a homogeneous nuclear pattern, consistent with the original observation in mixed B6/129 background $CD45^{W/W}$ mice (Figure 4A). In contrast, $CD45^{W/W}/Dnase1^{-/-}$ mice developed no significant autoantibody titers up to age 10 months (Figure 4B). IgG anti-dsDNA production did not reflect a polyclonal gammopathy as total IgG levels in all mutants were comparable to wild type (data not shown).

We noted that as early as 8 weeks of age, the $CD45^{W/W}/Pep^{-/-}$ mice developed lymphadenopathy and splenomegaly which was progressive with time and greatly exceeded the mild lymphoproliferation evident in each of the single mutants (Figure 4C). Lymph node (LN) absolute cell counts were variably elevated among the aging cohort, with some reaching 10-fold normal levels by six months of age (Figure 4D). The lymphadenopathy was generally out of proportion to the degree of splenomegaly observed, suggesting a lymphoid predominant dysregulation of the hematopoietic compartment (Figure 4C and data not shown). In contrast, LN size, LN cell number and spleen weights in $CD45^{W/W}/Dnase1^{-/-}$ mice were comparable to values in $CD45^{W/W}$ single mice (age 10 months, data not shown). No excess mortality was observed out to 10 months of age. Subsequent results and analysis in this paper will be limited to the $CD45^{W/W}/Pep^{-/-}$ mice.

Although $CD45^{W/W}/Pep^{-/-}$ mice displayed reduced body weights as early as 6 months of age, overt morbidity and mortality was evident only by 10 months of age. We noted onset of

proteinuria and subsequent mortality in a subset of mice by 10 months of age (data not shown). By 12 months of age, 33% of our initial cohort of $CD45^{W/W}/Pep^{-/-}$ mice had died (N=15). The remaining genotypes had normal life expectancy.

We next attempted to define the cause of death in the $CD45^{W/W}/Pep^{-/-}$ mice. The surviving $CD45^{W/W}/Pep^{-/-}$ mice at age 12 months were small, had variable degrees of proteinuria, and had pale and nodular kidneys on gross pathology (data not shown). Other major organs appeared grossly normal. Histologic examination of $CD45^{W/W}/Pep^{-/-}$ kidneys revealed marked abnormalities including perivascular lymphocytic infiltrates, interstitial lymphocytic infiltrates and hypercellular glomeruli with evidence of segmental sclerosis (Figure 4E–H). $CD45^{W/W}$ single mutant mice showed very mild evidence of similar abnormalities in kidney histology. Both $CD45^{W/W}/Pep^{-/-}$ and $CD45^{W/W}$ single mutants had evidence of perivascular infiltrates in lung and liver at 12 months of age to a comparable extent, but these infiltrates did not appear to extend into organ parenchyma (data not shown). We conclude that renal failure due to glomerulonephritis was the likely cause of premature mortality in the $CD45^{W/W}/Pep^{-/-}$ mice.

Given the presence of lymphoproliferation, autoantibody production, autoimmune kidney pathology and mortality, we conclude that the $CD45^{W/W}/Pep^{-/-}$ mice develop a lupus-like disease in a partially penetrant fashion that recapitulates the original disease phenotype observed on the B6/129 mixed background (31). Neither $CD45^{W/W}$, nor $Pep^{-/-}$ single mutant mice developed lupus-like autoimmunity over the course of 12 months of observation. $CD45^{W/W}/Dnase1^{-/-}$ mice displayed no evidence of genetic cooperation or frank autoimmunity.

Double mutant mice develop polyclonal T cell activation and an expanded effector/memory compartment

To begin to understand the mechanism by which overt autoimmunity arises in the $CD45^{W/W}/Pep^{-/-}$ double mutant mice, we assessed the cellular immune phenotype. The enlarged lymphoid compartment in double mutant mice was not due to the expansion of a single hematopoietic lineage. Double mutant lymph nodes contained relatively preserved ratios of T and B cells (Figure 5A). The CD4 : CD8 peripheral T cell ratio was increased consistently in the double mutants and less so in each single mutant relative to WT in both LN and spleen (Figure 5B and data not shown). This ratio shift was evident as early as 6 weeks of age and persisted throughout the observation period (12 months).

The most marked cellular phenotype was the progressive expansion of the CD4 and CD8 T cell memory/effector compartments in double mutant mice, as identified by CD44 and CD62L surface markers (Figure 5C, 5E). A more subtle version of this phenotype is evident in each single mutant. This phenomenon was observed in the spleen as well as the lymph node T cell compartment, occurred early, and progressed with time (Figure 5D, 5F and data not shown). The activation marker CD69 was upregulated in double mutant CD4 and CD8 T cells and to a lesser extent in each single mutant (Figure 5G, 5H).

B cell development and activation are not influenced by Pep deficiency

In contrast to T cells, B cells upregulated activation markers such as CD69 as well as CD80/86 in $CD45^{W/W}$ and double mutant mice, but not in $Pep^{-/-}$ mice. The activation status of B cells at age 2 months was matched in $CD45^{W/W}$ and double mutant mice, but by 6 months of age, double mutant mice further upregulated B cell activation markers (Figure 6A and data not shown). The plasma cell compartment identified by cell surface CD138 expression was expanded in $CD45^{W/W}$ and double mutant spleens to a similar extent, while $Pep^{-/-}$ mice resembled WT (Figure 6B).

BCR signaling is critical for B cell development and is characteristically perturbed in $CD45^{W/W}$ mice (32). Using markers CD21, CD23, IgM, IgD, and AA4.1, we found that double mutant mice precisely phenocopied the $CD45^{W/W}$ splenic B cell phenotype with expansion of newly formed (NF) / transitional (T1/T2) B cell subsets at the expense of the mature follicular (FO) B cell subset as previously described (Figure 6C–F and data not shown) (32). Consistent with the previously reported expansion of B1 B cells in $CD45^{W/W}$ mice, double mutant and $CD45^{W/W}$ mice have increased total serum IgM levels (data not shown) (32). In contrast, the $Pep^{-/-}$ splenic B cell phenotype resembled WT, consistent with the absence of Pep expression in B cells.

B cell receptor signaling is not influenced by Pep deficiency

Because double mutant mice uniquely develop a break in B cell tolerance as indicated by autoantibody production, we first sought to define the cell intrinsic contribution of the B cell lineage to this phenotype by assessing BCR signaling directly. Double mutant and $CD45^{W/W}$ B cells in spleen and lymph nodes were found to be hyper-responsive to in vitro BCR stimulation as assessed by Erk phosphorylation. Notably, $Pep^{-/-}$ B cells responded like WT B cells, while double mutant B cells responded like $CD45^{W/W}$ B cells with no evidence of unmasked synergy in the double mutant (Figure 7A). We identified similar trends with alternate readouts downstream of BCR ligation such as calcium flux, activation marker upregulation, and CFSE dilution (Figure 7B and data not shown). These data are compatible with the absence of detectable Pep expression in B cells and unperturbed B cell development in $Pep^{-/-}$ mice. Consistent with these data, a B cell signaling phenotype was not previously demonstrated in $Pep^{-/-}$ mice (17).

Although lymph node B cells represent a relatively uniform, predominantly mature phenotype, splenic B cells include multiple developmental stages, each with unique signaling thresholds. To define the precise stage of B cell development at which $CD45^{W/W}$ contributes to hyper-responsiveness, we assessed BCR-induced Erk phosphorylation in conjunction with B cell surface staining by flow cytometry. Surprisingly, signaling was relatively normal in newly formed (NF) B cells of all genotypes, but follicular mature (FO) B cells from $CD45^{W/W}$ and double mutants were markedly hyper-responsive, consistent with the lymph node data (Figure 7C).

We suggest from these data that in double mutant mice, the CD45 E613R `Wedge' allele contributes to a B cell tolerance break at the follicular mature stage of development in a cell intrinsic fashion, while Pep deficiency does so in a cell extrinsic fashion.

Pep deficiency and CD45 E613R cooperate to enhance TCR signaling in the thymus

To understand the contribution of Pep deficiency to the double mutant phenotype, we examined the T cell lineage, where Pep is predominantly expressed. Thymocyte development was grossly intact as assessed by double negative, double positive, and single positive subset compartment size (data not shown). Double negative subsets 1 through 4 as assessed by CD44 and CD25 surface markers were also unperturbed without evidence of abnormalities in beta-selection (data not shown).

Both $Pep^{-/-}$ and $CD45^{W/W}$ mice have been previously independently crossed to TCR transgenes (H–Y, OT-2 and DO11.10), revealing increased positive selection in each background (17); (Hermiston et al, manuscript in preparation). We therefore characterized the cell surface phenotype of double positive (DP) thymocytes. We noted upregulation of CD5 and CD69 in double mutant mice relative to WT and less so in each single mutant (Figure 8A and data not shown). These markers are well-established correlates of TCR signal strength and

suggest that $CD45^{W/W}$ and $Pep^{-/-}$ cooperate in a cell intrinsic manner at the DP thymocyte stage of T cell development (38).

We tested this hypothesis by stimulating the TCR on DP thymocytes in vitro and assessed Erk phosphorylation and calcium flux by flow cytometry. These studies revealed subtle hyper-responsiveness in DP thymocytes of each single mutant and a uniquely heightened response in double mutant mice (Figure 8B and 8C). This alteration in signaling was not due to any downstream rewiring as PMA and ionomycin produced comparable Erk phosphorylation and calcium flux, respectively (Figure 8B and data not shown).

CD45 E613R does not contribute to TCR hyper-responsiveness in peripheral T cells

Although $Pep^{-/-}$ and $CD45^{W/W}$ cooperate to enhance TCR signaling in double mutant DP thymocytes, such a perturbation should in theory increase both positive and negative selection, resulting in enhanced rather than impaired central tolerance. This conclusion led us to turn our attention to peripheral T cells in order to understand in what cell type and at which stage the two mutations cooperate to break tolerance. Because peripheral T cell subsets have qualitatively distinct signaling properties, we systematically interrogated TCR signaling in naïve, memory and effector CD4 and CD8 T cells. We initially hypothesized that the unique memory/effector phenotype in double mutant mice was due to uniquely enhanced peripheral T cell signaling in double mutant mice. To our surprise we found that this was not the case. We further discovered that the CD45 E613R allele makes no significant contribution to the TCR signaling in peripheral T cells.

Because of the unequal size and signaling properties of $CD44^{hi}$ memory and $CD44^{lo}$ naïve T cell subsets in our four genotypes, we compared responsiveness to TCR ligation separately in naïve and memory T cell subsets by gating on surface CD44 expression while evaluating Erk phosphorylation by flow cytometry. This revealed no substantial differences in naïve or memory T cell responsiveness among the four genotypes, except among naive CD8+ naïve ($CD44^{lo}$) T cells where we observed consistent and equivalent TCR hyper-responsiveness in $Pep^{-/-}$ and double mutant mice (Figure 8D).

We confirmed these observations by examining an event further downstream of TCR stimulation. We evaluated CD69 upregulation specifically in $CD44^{lo}$ gated naïve T cells. Double mutant CD8 T cells consistently responded comparably to $Pep^{-/-}$ T cells, while $CD45^{W/W}$ T cells responded comparably to WT (data not shown). Among CD8 T cells, we observed at most a 2-fold shift in the dose response curve to anti-CD3 stimulation, suggesting that $Pep^{-/-}$ alters signal sensitivity very subtly in the naïve T cell compartment. Other readouts such as calcium flux and CFSE dilution failed to reveal consistent differences between the four genotypes, possibly because they rely upon collective signal from a heterogeneous pool of T cells. To our surprise, no readout of TCR signal strength revealed hyper-responsiveness in $CD45^{W/W}$ naïve or pooled peripheral T cells.

To explain the accumulation of memory/effector T cells in double mutant mice in the absence of a unique double mutant naïve T cell phenotype, we hypothesized a stage specific influence of $CD45^{W/W}$ and $Pep^{-/-}$ alleles on effector T cells, rather than naïve or memory T cells. We stimulated the TCR of in vitro generated CD4 and CD8 effector T cells from all four genotypes and assessed Erk phosphorylation both by flow and by western blotting. We found subtle and comparable hyper-responsiveness in $Pep^{-/-}$ and double mutant CD4 effectors, but not in CD8 effectors (Figure 8E). Consistent with these observations, Hasegawa et al. have previously characterized the T cell phenotype in $Pep^{-/-}$ mice, reporting hyper-responsiveness in the “memory/effector” compartment in the absence of a naïve T cell phenotype (17). Again, no impact of the CD45 E613R wedge allele was observed, implying that the progressive

accumulation of memory/effector T cells in double mutant animals cannot be accounted for by a purely T cell intrinsic signaling phenotype.

Discussion

Function of PTPN22

Our model is the first reported autoimmune disease phenotype for *PTPN22* in mice and helps to clarify both the mechanism by which *PTPN22* functions as a general autoimmune susceptibility locus in humans, and the genetic context in which it might do so. The R620W polymorphism disrupts the critical interaction of Pep/Lyp with Csk and thereby impairs Pep's ability to effectively access its target Lck (2). Prior studies of the functional consequences of this polymorphism have led to conflicting results. The R620W variant was reported to have slightly enhanced enzymatic activity in an vitro phosphatase assay (19). Studies of primary human cells harboring the risk allele and prior overexpression studies in Jurkat cells suggest as well that this variant impairs TCR signaling, implying a gain of function (19,20). Several other studies using primary human cells from patients with autoimmune disease are more difficult to interpret (19,21,22). However, previous Jurkat studies have failed to define fold overexpression or dose response, and function was not assessed in the context of Csk (19).

We find that wild type murine Pep or human Lyp overexpression in the context of Csk clearly exhibits cooperative inhibition of proximal TCR signaling and does so more effectively than the R620W allele. Our studies reflect a more physiologic stoichiometry than prior work, and control explicitly for expression level and overexpression artifact. These differences may explain discrepancies with prior reports. Furthermore, we can now exclude the possibility that human and murine orthologs may exhibit functional differences in this context. It remains a formal possibility that Pep and/or Lyp regulates signaling pathways other than those downstream of the antigen receptor, and targets additional as yet unidentified substrates.

Clues to the functional impact of this polymorphism on disease pathogenesis can be gleaned from several human genetic studies. The *PTPN22* R620W polymorphism is a risk factor not simply for autoimmune disease characterized by pathogenic autoantibody production (such as SLE, Grave's disease, and myasthenia gravis), but particularly for autoantibody-positive disease variants (5). The risk allele is specifically associated with seropositive and anti-cyclic citrullinated peptide (CCP) antibody-positive RA and not with seronegative disease (5,39, 40). Indeed, there is no positive association between the risk allele and either inflammatory bowel disease or multiple sclerosis, neither of which have autoantibodies as a significant pathogenic feature (5,39). Interestingly, the non-risk allele of *PTPN22* is associated with tuberculosis, not only suggesting a selective evolutionary pressure to account for the prevalence of the risk allele, but supplying hints of a mechanism (41). Certainly, hyper-responsive T cells such as those in $Pep^{-/-}$ mice might plausibly mediate this resistance. The host response of these mice in the context of infection has not been defined.

Unambiguous resolution of whether the R620W allele is a hypo-or hypermorph must address both the genetic and environmental heterogeneity that confounds functional studies of primary human cells and the limitations of phosphatase overexpression in cell lines. Certainly a gain of function Pep/Lyp allele could impair negative selection in the thymus or Treg function in the periphery. Both types of perturbations can provoke autoimmune disease in mice (and rarely in humans) (42,43). Alternatively, we have shown that a hypomorphic *PTPN22* variant in T cells might serve to drive hyper-responsive B cells to break tolerance in the periphery and produce autoantibodies, as we see in the $CD45^{W/W}/Pep^{-/-}$ model. The association of the R620W allele almost exclusively with autoantibody-positive diseases and variants could be understood in light of this mechanism.

Cellular mechanism of disease

Although we have provided evidence that the human risk allele of *PTPN22* is a hypomorph, Pep-deficiency on the B6 background fails to break tolerance independently. Here we demonstrate that it cooperates with the CD45 E613R genetic background to provoke overt autoimmune disease. By generating disease in the context of a bona fide human susceptibility allele, our model sheds light on early pathogenesis of human autoimmune disease.

In our analysis of this model, we sought to identify cell intrinsic and cell extrinsic phenotypes in order to establish, respectively, direct and indirect events in disease pathogenesis. We reasoned that the cell-intrinsic effects of the genetic perturbations in our model ought directly and primarily to influence antigen-receptor signal transduction since Pep and CD45 reciprocally regulate the SFKs, critical proximal mediators of these signals.

We have demonstrated enhanced TCR signal sensitivity at the double positive stage of thymic development. The critical central tolerance mechanism of negative selection remains intact, preventing autoreactive clones from escaping to the periphery. As a result of enhanced positive selection, the T cell repertoire may be perturbed in favor of non-autoreactive, weak affinity receptors and expanded numbers of Treg cells. Neither change would be expected to contribute to a break in self tolerance. Abnormally selected, weak affinity TCRs coupled to very subtly hyper-responsive peripheral T cells ought not to cross the threshold for inappropriate activation. Indeed, other autoimmune mouse models with altered T cell repertoires that contribute to disease show evidence of impaired rather than enhanced selection in the thymus (42–45). Therefore we suggest that the thymic phenotype is not likely to contribute to the tolerance break we detect in our model.

We have shown that Pep is expressed in T cells and Pep-deficiency makes a lone contribution to peripheral TCR hyper-responsiveness in double mutant mice. This suggests that the CD45 E613R allele does not exert a significant cell-intrinsic effect in peripheral T cells. In contrast, the accumulation of effector/memory T cells in the double mutant mice is significantly accelerated relative to either mutation in isolation. We conclude that the $CD45^{W/W}$ microenvironment makes a purely cell extrinsic contribution to this “indirect” T cell phenotype. The $CD45^{W/W}$ contribution could represent the influence of myeloid and/or B cell compartments. Other murine models of lupus have demonstrated that both scenarios are possible (46–48). The non-T cell compartment may secrete cytokines or provide costimulation to drive T cell differentiation. It is also possible, although less likely, that altered T cell repertoire in the double mutant mice contributes to these “emergent” T cell phenotypes.

BCR signaling in the double mutant mice, in contrast, is influenced exclusively by the $CD45^{W/W}$ genetic background, and is specifically perturbed at the “final” follicular mature stage of B cell development. We therefore conclude that unique B cell phenotypes seen only in the double mutant mouse such as augmented polyclonal activation, B cell compartment expansion and, of course, autoantibody production are partially B cell extrinsic in our model, driven by $Pep^{-/-}$ T cells. Others have demonstrated that memory/effector T cells have pathogenic potential, possibly by interacting with B cells via CD40L or ICOS(49). Indeed, $Pep^{-/-}$ mice develop spontaneous germinal centers despite the absence of a B cell-intrinsic signaling phenotype, suggesting a role for $Pep^{-/-}$ effector T helper cells in promoting B cell differentiation in this model. Hyper-responsive follicular mature $CD45^{W/W}$ B cells are ideally situated to cooperate productively in such a context. These genetic interactions between Pep deficiency and the $CD45^{W/W}$ background bypass tight central tolerance mechanisms and lead to a tolerance break only in the periphery. Indeed previous analysis of $CD45^{W/W}$ B cells in the context of the Ig HEL transgene confirm that central negative selection of B cells is not only intact, but is enhanced (32).

Numerous spontaneous and engineered models of lupus in mice have also demonstrated the critical role of hyper-responsive BCR signaling in disease pathogenesis (34,35,50). Substantial evidence suggests that primary human B cells from patients with SLE are similarly hyper-responsive and that this phenotype is independent of disease activity and treatment (33). Recent data from whole genome association studies of SLE in humans have identified genes in the BCR signaling pathway, including the B cell-specific src family kinase Blk, and the adaptor BANK1 (51,52). In this regard, the B cell hyper-responsiveness of the CD45 E613R mice is a representative model of human lupus pathogenesis.

Our lupus model is characterized by hyper-responsive T and B cells. Each cellular phenotype taken independently is insufficient to break tolerance, but in combination, emergent phenotypes such as polyclonal T and B cell activation and frank autoimmune disease develop. This is reminiscent of the genetic dissection of the polygenic spontaneous murine lupus model NZB/W(53). Given the significance of the *PTPN22* genetic locus in human autoimmunity, our data suggests that similar analysis may be valid in human disease. Indeed, given the subtlety of the risk conferred by the R620W allele in human disease, it is not surprising that cooperating functional phenotypes such as B cell hyper-reactivity may be required to break tolerance.

Conclusion

Although most common human autoimmune diseases are complex polygenic traits, studies of such processes in mice using reverse genetics has traditionally involved creating models in which a single overwhelming genetic lesion provokes disease. These models are invaluable for understanding late disease pathogenesis and testing therapeutic interventions. However, as whole genome scans come of age and identify multiple subtle human genetic polymorphisms which cooperate in a very complex fashion, we need a novel approach to understand how such polymorphisms function and in which contexts.

Here we have demonstrated that a loss of function *PTPN22* gene product in T cells recapitulates the R620W human risk allele and can cooperate with hyper-responsive B cells to provoke autoantibody production and a lupus-like autoimmune disease, reminiscent of its human disease associations.

Acknowledgments

We would like to thank Al Roque for assistance with animal husbandry and members of the Weiss lab for helpful discussions. We are grateful to Jaime Schoenborn for generating Csk constructs and assisting with transfection experiments, and to Lyn Hsu for help with cloning.

This work was supported in part by grants from the NIH (POI AI 035297, to AW and MH) and from the Arthritis Foundation (to JZ).

Abbreviations used

TCR, T cell receptor
BCR, B cell receptor
SFK, Src family kinase
ITAM, immune tyrosine activating motif
PRS, proline-rich sequence
RA, rheumatoid arthritis
SLE, systemic lupus erythematosus
B6, C57BL/6
WT, wild type
DP, double positive
ANA, anti-nuclear antibody

References

1. Begovich AB, Carlton VE, Honigberg LA, Schrodi SJ, Chokkalingam AP, Alexander HC, Ardlie KG, Huang Q, Smith AM, Spoerke JM, Conn MT, Chang M, Chang SY, Saiki RK, Catanese JJ, Leong DU, Garcia VE, McAllister LB, Jeffery DA, Lee AT, Batliwalla F, Remmers E, Criswell LA, Seldin MF, Kastner DL, Amos CI, Sninsky JJ, Gregersen PK. A missense single-nucleotide polymorphism in a gene encoding a protein tyrosine phosphatase (PTPN22) is associated with rheumatoid arthritis. Am J Hum Genet 2004;75:330–337. [PubMed: 15208781]
2. Bottini N, Musumeci L, Alonso A, Rahmouni S, Nika K, Rostamkhani M, MacMurray J, Meloni GF, Lucarelli P, Pellecchia M, Eisenbarth GS, Comings D, Mustelin T. A functional variant of lymphoid tyrosine phosphatase is associated with type I diabetes. Nat Genet 2004;36:337–338. [PubMed: 15004560]
3. Kyogoku C, Langefeld CD, Ortmann WA, Lee A, Selby S, Carlton VE, Chang M, Ramos P, Baechler EC, Batliwalla FM, Novitzke J, Williams AH, Gillett C, Rodine P, Graham RR, Ardlie KG, Gaffney PM, Moser KL, Petri M, Begovich AB, Gregersen PK, Behrens TW. Genetic association of the R620W polymorphism of protein tyrosine phosphatase PTPN22 with human SLE. Am J Hum Genet 2004;75:504–507. [PubMed: 15273934]
4. Genome-wide association study of 14,000 cases of seven common diseases and 3,000 shared controls. Nature 2007;447:661–678. [PubMed: 17554300]
5. Gregersen PK, Lee HS, Batliwalla F, Begovich AB. PTPN22: setting thresholds for autoimmunity. Semin Immunol 2006;18:214–223. [PubMed: 16731003]
6. Plenge RM, Seielstad M, Padyukov L, Lee AT, Remmers EF, Ding B, Liew A, Khalili H, Chandrasekaran A, Davies LR, Li W, Tan AK, Bonnard C, Ong RT, Thalamuthu A, Pettersson S, Liu C, Tian C, Chen WV, Carulli JP, Beckman EM, Altshuler D, Alfredsson L, Criswell LA, Amos CI, Seldin MF, Kastner DL, Klareskog L, Gregersen PK. TRAF1-C5 as a risk locus for rheumatoid arthritis--a genomewide study. N Engl J Med 2007;357:1199–1209. [PubMed: 17804836]
7. MacGregor AJ, Snieder H, Rigby AS, Koskenvuo M, Kaprio J, Aho K, Silman AJ. Characterizing the quantitative genetic contribution to rheumatoid arthritis using data from twins. Arthritis Rheum 2000;43:30–37. [PubMed: 10643697]
8. Cohen S, Dadi H, Shaoul E, Sharfe N, Roifman CM. Cloning and characterization of a lymphoid-specific, inducible human protein tyrosine phosphatase, Lyp. Blood 1999;93:2013–2024. [PubMed: 10068674]
9. Matthews RJ, Bowne DB, Flores E, Thomas ML. Characterization of hematopoietic intracellular protein tyrosine phosphatases: description of a phosphatase containing an SH2 domain and another enriched in proline-, glutamic acid-, serine-, and threonine-rich sequences. Mol Cell Biol 1992;12:2396–2405. [PubMed: 1373816]
10. Cloutier JF, Veillette A. Cooperative inhibition of T-cell antigen receptor signaling by a complex between a kinase and a phosphatase. J Exp Med 1999;189:111–121. [PubMed: 9874568]
11. Gjorloff-Wingren A, Saxena M, Williams S, Hammi D, Mustelin T. Characterization of TCR-induced receptor-proximal signaling events negatively regulated by the protein tyrosine phosphatase PEP. Eur J Immunol 1999;29:3845–3854. [PubMed: 10601992]
12. Iwashima M, Irving BA, van Oers NS, Chan AC, Weiss A. Sequential interactions of the TCR with two distinct cytoplasmic tyrosine kinases. Science 1994;263:1136–1139. [PubMed: 7509083]
13. Cloutier JF, Veillette A. Association of inhibitory tyrosine protein kinase p50csk with protein tyrosine phosphatase PEP in T cells and other hemopoietic cells. Embo J 1996;15:4909–4918. [PubMed: 8890164]
14. Chow LM, Fournel M, Davidson D, Veillette A. Negative regulation of T-cell receptor signalling by tyrosine protein kinase p50csk. Nature 1993;365:156–160. [PubMed: 8371758]
15. Kawabuchi M, Satomi Y, Takao T, Shimonishi Y, Nada S, Nagai K, Tarakhovsky A, Okada M. Transmembrane phosphoprotein Cbp regulates the activities of Src-family tyrosine kinases. Nature 2000;404:999–1003. [PubMed: 10801129]
16. Brdicka T, Pavlistova D, Leo A, Bruyns E, Korinek V, Angelisova P, Scherer J, Shevchenko A, Hilgert I, Cerny J, Drbal K, Kuramitsu Y, Kornacker B, Horejsi V, Schraven B. Phosphoprotein associated with glycosphingolipid-enriched microdomains (PAG), a novel ubiquitously expressed

transmembrane adaptor protein, binds the protein tyrosine kinase csk and is involved in regulation of T cell activation. J Exp Med 2000;191:1591–1604. [PubMed: 10790433]

17. Hasegawa K, Martin F, Huang G, Tumas D, Diehl L, Chan AC. PEST domain-enriched tyrosine phosphatase (PEP) regulation of effector/memory T cells. Science 2004;303:685–689. [PubMed: 14752163]
18. Arimura Y, Vang T, Tautz L, Williams S, Mustelin T. TCR-induced downregulation of protein tyrosine phosphatase PEST augments secondary T cell responses. Mol Immunol 2008;45:3074–3084. [PubMed: 18457880]
19. Vang T, Congia M, Macis MD, Musumeci L, Orru V, Zavattari P, Nika K, Tautz L, Tasken K, Cucca F, Mustelin T, Bottini N. Autoimmune-associated lymphoid tyrosine phosphatase is a gain-of-function variant. Nat Genet 2005;37:1317–1319. [PubMed: 16273109]
20. Rieck M, Arechiga A, Onengut-Gumuscu S, Greenbaum C, Concannon P, Buckner JH. Genetic variation in PTPN22 corresponds to altered function of T and B lymphocytes. J Immunol 2007;179:4704–4710. [PubMed: 17878369]
21. Lefvert AK, Zhao Y, Ramanujam R, Yu S, Pirskanen R, Hammarstrom L. PTPN22 R620W promotes production of anti-AChR autoantibodies and IL-2 in myasthenia gravis. J Neuroimmunol 2008;197:110–113. [PubMed: 18533277]
22. Aarnisalo J, Treszl A, Svec P, Marttila J, Oling V, Simell O, Knip M, Korner A, Madacsy L, Vasarhelyi B, Ilonen J, Hermann R. Reduced CD4(+)T cell activation in children with type 1 diabetes carrying the PTPN22/Lyp 620Trp variant. J Autoimmun 2008;31:13–21. [PubMed: 18299186]
23. Hermiston ML, Xu Z, Weiss A. CD45: a critical regulator of signaling thresholds in immune cells. Annu Rev Immunol 2003;21:107–137. [PubMed: 12414720]
24. Byth KF, Conroy LA, Howlett S, Smith AJ, May J, Alexander DR, Holmes N. CD45-null transgenic mice reveal a positive regulatory role for CD45 in early thymocyte development, in the selection of CD4+CD8+ thymocytes, and B cell maturation. J Exp Med 1996;183:1707–1718. [PubMed: 8666928]
25. Kishihara K, Penninger J, Wallace VA, Kundig TM, Kawai K, Wakeham A, Timms E, Pfeffer K, Ohashi PS, Thomas ML, et al. Normal B lymphocyte development but impaired T cell maturation in CD45-exon6 protein tyrosine phosphatase-deficient mice. Cell 1993;74:143–156. [PubMed: 8334701]
26. Kung C, Pingel JT, Heikinheimo M, Klemola T, Varkila K, Yoo LI, Vuopala K, Poyhonen M, Uhari M, Rogers M, Speck SH, Chatila T, Thomas ML. Mutations in the tyrosine phosphatase CD45 gene in a child with severe combined immunodeficiency disease. Nat Med 2000;6:343–345. [PubMed: 10700239]
27. Mee PJ, Turner M, Basson MA, Costello PS, Zamoyska R, Tybulewicz VL. Greatly reduced efficiency of both positive and negative selection of thymocytes in CD45 tyrosine phosphatase-deficient mice. Eur J Immunol 1999;29:2923–2933. [PubMed: 10508267]
28. Tchilian EZ, Beverley PC. Altered CD45 expression and disease. Trends Immunol 2006;27:146–153. [PubMed: 16423560]
29. Desai DM, Sap J, Schlessinger J, Weiss A. Ligand-mediated negative regulation of a chimeric transmembrane receptor tyrosine phosphatase. Cell 1993;73:541–554. [PubMed: 8490965]
30. Majeti R, Bilwes AM, Noel JP, Hunter T, Weiss A. Dimerization-induced inhibition of receptor protein tyrosine phosphatase function through an inhibitory wedge. Science 1998;279:88–91. [PubMed: 9417031]
31. Majeti R, Xu Z, Parslow TG, Olson JL, Daikh DI, Killeen N, Weiss A. An inactivating point mutation in the inhibitory wedge of CD45 causes lymphoproliferation and autoimmunity. Cell 2000;103:1059–1070. [PubMed: 11163182]
32. Hermiston ML, Tan AL, Gupta VA, Majeti R, Weiss A. The juxtamembrane wedge negatively regulates CD45 function in B cells. Immunity 2005;23:635–647. [PubMed: 16356861]
33. Liossis SN, Kovacs B, Dennis G, Kammer GM, Tsokos GC. B cells from patients with systemic lupus erythematosus display abnormal antigen receptor-mediated early signal transduction events. J Clin Invest 1996;98:2549–2557. [PubMed: 8958217]

34. Mohan C, Morel L, Yang P, Wakeland EK. Genetic dissection of systemic lupus erythematosus pathogenesis: Sle2 on murine chromosome 4 leads to B cell hyperactivity. J Immunol 1997;159:454–465. [PubMed: 9200486]
35. Zouali M, Sarmay G. B lymphocyte signaling pathways in systemic autoimmunity: implications for pathogenesis and treatment. Arthritis Rheum 2004;50:2730–2741. [PubMed: 15457440]
36. Wu J, Katrekar A, Honigberg LA, Smith AM, Conn MT, Tang J, Jeffery D, Mortara K, Sampang J, Williams SR, Buggy J, Clark JM. Identification of substrates of human protein-tyrosine phosphatase PTPN22. J Biol Chem 2006;281:11002–11010. [PubMed: 16461343]
37. Napirei M, Karsunky H, Zevnik B, Stephan H, Mannherz HG, Moroy T. Features of systemic lupus erythematosus in Dnase1-deficient mice. Nat Genet 2000;25:177–181. [PubMed: 10835632]
38. Azzam HS, Grinberg A, Lui K, Shen H, Shores EW, Love PE. CD5 expression is developmentally regulated by T cell receptor (TCR) signals and TCR avidity. J Exp Med 1998;188:2301–2311. [PubMed: 9858516]
39. Chung SA, Criswell LA. PTPN22: its role in SLE and autoimmunity. Autoimmunity 2007;40:582–590. [PubMed: 18075792]
40. Karlson EW, Chibnik LB, Cui J, Plenge RM, Glass RJ, Maher NE, Parker A, Roubenoff R, Izmailova E, Coblyn JS, Weinblatt ME, Shadick NA. Associations between human leukocyte antigen, PTPN22, CTLA4 genotypes and rheumatoid arthritis phenotypes of autoantibody status, age at diagnosis and erosions in a large cohort study. Ann Rheum Dis 2008;67:358–363. [PubMed: 17666451]
41. Gomez LM, Anaya JM, Martin J. Genetic influence of PTPN22 R620W polymorphism in tuberculosis. Hum Immunol 2005;66:1242–1247. [PubMed: 16690411]
42. Anderson MS, Venanzi ES, Klein L, Chen Z, Berzins SP, Turley SJ, von Boehmer H, Bronson R, Dierich A, Benoist C, Mathis D. Projection of an immunological self shadow within the thymus by the aire protein. Science 2002;298:1395–1401. [PubMed: 12376594]
43. Sakaguchi N, Takahashi T, Hata H, Nomura T, Tagami T, Yamazaki S, Sakihama T, Matsutani T, Negishi I, Nakatsuru S, Sakaguchi S. Altered thymic T-cell selection due to a mutation of the ZAP-70 gene causes autoimmune arthritis in mice. Nature 2003;426:454–460. [PubMed: 14647385]
44. Siggs OM, Miosge LA, Yates AL, Kucharska EM, Sheahan D, Brdicka T, Weiss A, Liston A, Goodnow CC. Opposing functions of the T cell receptor kinase ZAP-70 in immunity and tolerance differentially titrate in response to nucleotide substitutions. Immunity 2007;27:912–926. [PubMed: 18093540]
45. Yoshitomi H, Sakaguchi N, Kobayashi K, Brown GD, Tagami T, Sakihama T, Hirota K, Tanaka S, Nomura T, Miki I, Gordon S, Akira S, Nakamura T, Sakaguchi S. A role for fungal {beta}-glucans and their receptor Dectin-1 in the induction of autoimmune arthritis in genetically susceptible mice. J Exp Med 2005;201:949–960. [PubMed: 15781585]
46. Zhu J, Liu X, Xie C, Yan M, Yu Y, Sobel ES, Wakeland EK, Mohan C. T cell hyperactivity in lupus as a consequence of hyperstimulatory antigen-presenting cells. J Clin Invest 2005;115:1869–1878. [PubMed: 15951839]
47. Lu Q, Lemke G. Homeostatic regulation of the immune system by receptor tyrosine kinases of the Tyro 3 family. Science 2001;293:306–311. [PubMed: 11452127]
48. Hibbs ML, Tarlinton DM, Armes J, Grail D, Hodgson G, Maglitto R, Stacker SA, Dunn AR. Multiple defects in the immune system of Lyn-deficient mice, culminating in autoimmune disease. Cell 1995;83:301–311. [PubMed: 7585947]
49. Vinuesa CG, Cook MC, Angelucci C, Athanasopoulos V, Rui L, Hill KM, Yu D, Domaschenz H, Whittle B, Lambe T, Roberts IS, Copley RR, Bell JI, Cornall RJ, Goodnow CC. A RING-type ubiquitin ligase family member required to repress follicular helper T cells and autoimmunity. Nature 2005;435:452–458. [PubMed: 15917799]
50. Chan OT, Madaio MP, Shlomchik MJ. B cells are required for lupus nephritis in the polygenic, Fas-intact MRL model of systemic autoimmunity. J Immunol 1999;163:3592–3596. [PubMed: 10490951]
51. Kozyrev SV, Abelson AK, Wojcik J, Zaghlool A, Linga Reddy MV, Sanchez E, Gunnarsson I, Svenungsson E, Sturfelt G, Jonsen A, Truedsson L, Pons-Estel BA, Witte T, D'Alfonso S, Barizzone N, Danieli MG, Gutierrez C, Suarez A, Junker P, Laustrup H, Gonzalez-Escribano MF, Martin J,

Abderrahim H, Alarcon-Riquelme ME. Functional variants in the B-cell gene BANK1 are associated with systemic lupus erythematosus. Nat Genet 2008;40:211–216. [PubMed: 18204447]

52. Hom G, Graham RR, Modrek B, Taylor KE, Ortmann W, Garnier S, Lee AT, Chung SA, Ferreira RC, Pant PV, Ballinger DG, Kosoy R, Demirci FY, Kamboh MI, Kao AH, Tian C, Gunnarsson I, Bengtsson AA, Rantapaa-Dahlqvist S, Petri M, Manzi S, Seldin MF, Ronnblom L, Syvanen AC, Criswell LA, Gregersen PK, Behrens TW. Association of Systemic Lupus Erythematosus with C8orf13-BLK and ITGAM-ITGAX. N Engl J Med. 2008
53. Morel L, Croker BP, Blenman KR, Mohan C, Huang G, Gilkeson G, Wakeland EK. Genetic reconstitution of systemic lupus erythematosus immunopathology with polycongenic murine strains. Proc Natl Acad Sci U S A 2000;97:6670–6675. [PubMed: 10841565]
54. Wofsy D, Seaman WE. Successful treatment of autoimmunity in NZB/NZW F1 mice with monoclonal antibody to L3T4. J Exp Med 1985;161:378–391. [PubMed: 3919141]

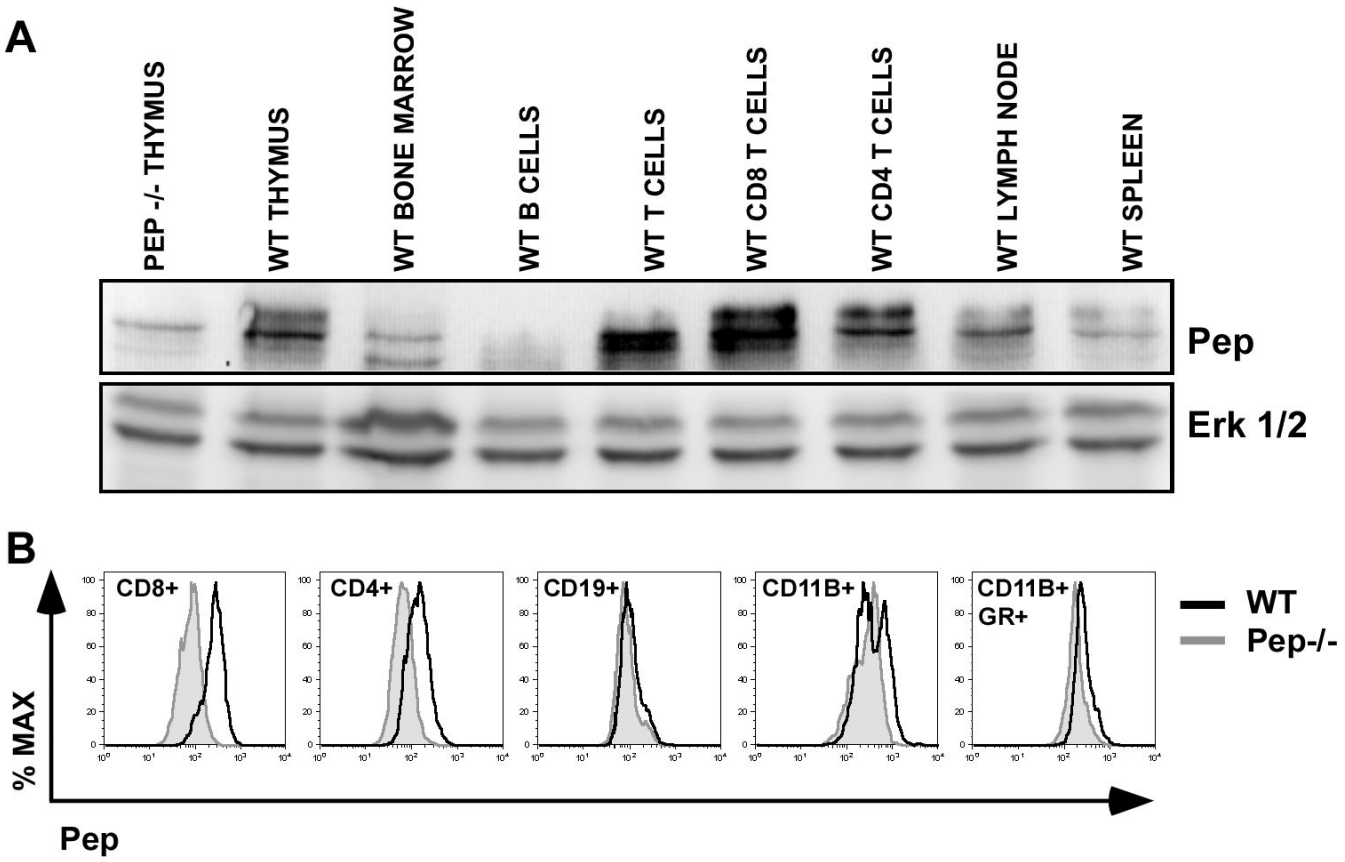

Figure 1.

Pep is expressed predominantly in T cells. (A) Whole cell lysates from wild type or $Pep^{-/-}$ animals were prepared from bone marrow, lymph nodes, spleen, thymus and MACS purified B cells, CD4 T cells, and CD8 T cells. Western blots were probed with polyclonal antibody recognizing Pep. The 105kD band corresponding to Pep is depicted and total Erk 1 and 2 is stained as a loading control. Analogous results with an independently generated Pep polyclonal antibody were obtained. (B) Histograms of lymph node or splenic subsets stained with polyclonal Pep antibody following permeabilization with saponin. Histograms of WT cells are represented by a black line while $Pep^{-/-}$ cells are represented by shaded gray histogram in each plot. Data presented are representative of three independent experiments.

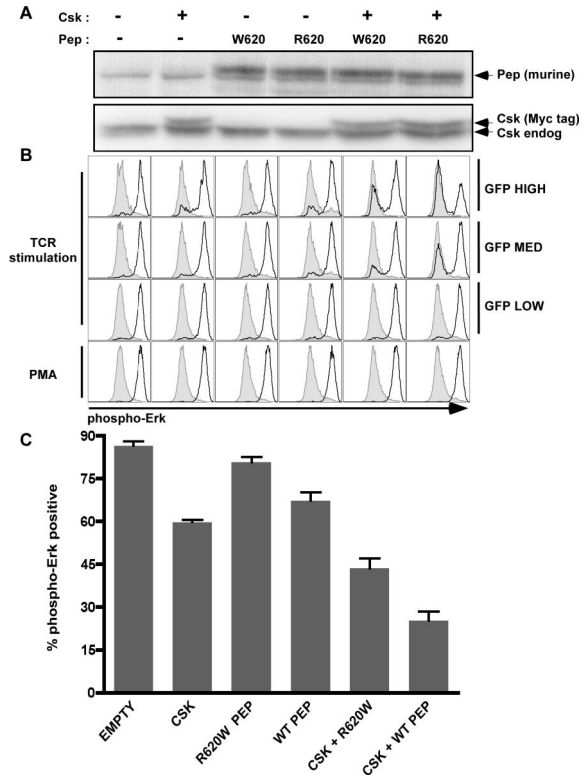

Figure 2.

The murine Pep `R620W' polymorphism functions as a hypomorph in the context of Csk. (A) Csk and wild type or R620W Pep were misexpressed in Jurkat cells together with GFP. Upper panel represents whole cell lysates of transfected cells probed for either Pep or Csk. Upper band in Pep blots represents murine Pep while lower band is non-specific background. Endogenous Lyp is not detected by this polyclonal antibody. (B) Histograms correspond to samples in (A) and represent intracellular phospho-Erk staining of transfected Jurkat cells stimulated throught the TCR by C305 or with PMA. GFP high, intermediate and low gating is shown. Gray histograms represent unstimulated transfectants for comparison. Black histograms represent stimulated transfectants as identified in (A). (C) Bar graph corresponding to samples generated and stimulated as in (A) and (B). % phospho-Erk positive cells are defined as % of cells which falls into the high expressing half of the bimodal histogram distributions in panel (B). Error bars represent SEM. Plots and western are representative of at least five independent experiments.

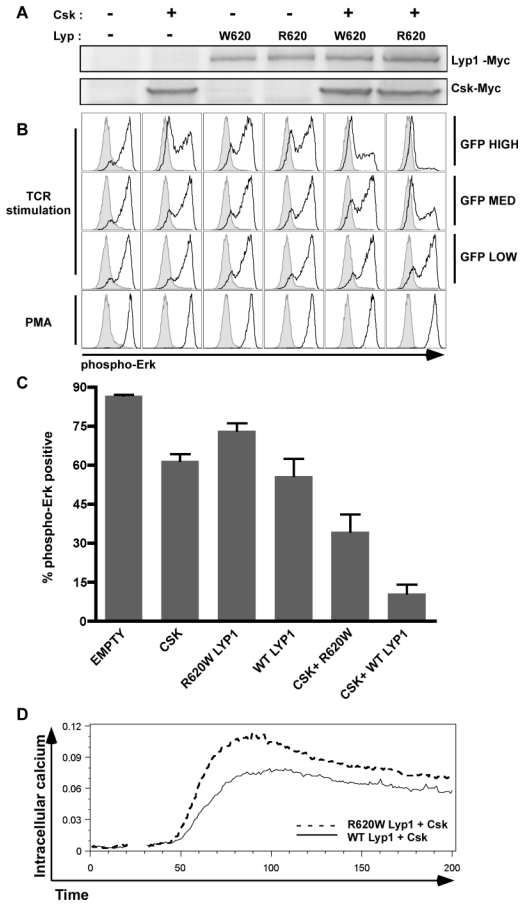

Figure 3.

The human Lyp1 R620W (T1858) polymorphism functions as a hypomorph in the context of Csk. (A) Csk and wild type or R620W Lyp1 were misexpressed in Jurkat cells together with GFP. Upper panel represents whole cell lysates of transfected cells probed for either myc-tagged Lyp1 or Csk. (B) Histograms correspond to samples in (A) and represent intracellular phospho-Erk staining of transfected Jurkat cells stimulated through the TCR by C305 or with PMA. GFP high, intermediate and low gating is shown. Gray histogram represent unstimulated transfectants for comparison. Black histograms represent stimulated transfectants as identified in (A). (C) Bar graph corresponding to samples generated and stimulated as in (A) and (B). % phospho-Erk positive cells are defined as in Figure 2(C). Error bars represent SEM. (D) Intracellular calcium levels of Lyp1/Csk transfected Jurkat cells (gated for co-transfected CD16). Fluo3/Fura Red ratio was monitored by flow cytometry before and after C305 stimulation of fluorophor-loaded transfectants. Solid line represents Csk+ Lyp1 R620*C1858 wild type allele. Dotted line represents Csk+ Lyp1 W620*T1858 risk allele. Plots, western, and calcium flux are representative of at least three independent experiments.

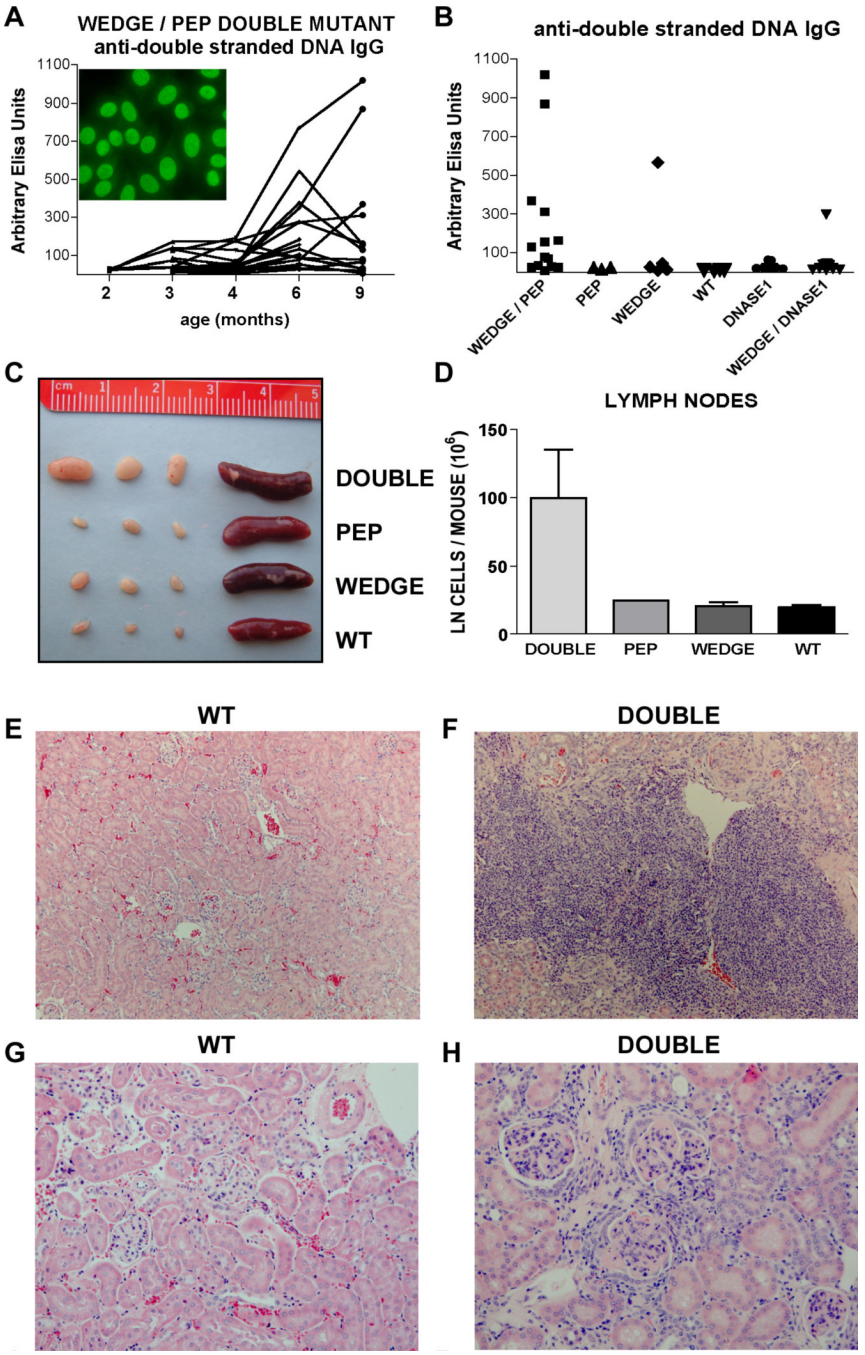

Figure 4.

$CD45^{w/w}/Pep^{-/-}$ double mutant mice develop lymphoproliferation and autoimmunity. Abbreviations apply to all subsequent figures : WEDGE = $CD45^{w/w}$; PEP = $Pep^{-/-}$; DNASE1 = $Dnase1^{-/-}$; DOUBLE = $CD45^{w/w}/Pep^{-/-}$ (A) ELISA for IgG autoantibodies reactive to double stranded DNA were performed on sera from $CD45^{w/w}/Pep^{-/-}$ double mutant mice at the indicated time points. Values represent individual mice and were normalized to average MRL/lpr serum = 1000 arbitrary elisa units. Inset represents anti-nuclear antibody staining pattern for 1:100 dilution of representative $CD45^{w/w}/Pep^{-/-}$ double mutant serum. (B) ELISA for IgG dsDNA autoantibodies of sera from various genotypes sampled at 9–10 months of age, normalized as in panel A. (C) Representative spleens and lymph nodes from genotypes at 5

months of age. (D) Lymph node absolute cell counts at 6 months of age. Values are the mean of three biological replicates +/− SEM. Similar results obtained at multiple time points ranging from 6 weeks to 12 months of age in at least 5 independent experiments each including 3 animals/genotype. (E) – (H) Hematoxylin and eosin staining of formalin fixed kidney sections from wild type and $CD45^{w/w}/Pep^{-/-}$ double mutant animals at 12 months of age. Representative specimens at 10X (E, F) and 20X (G, H) magnification are depicted.

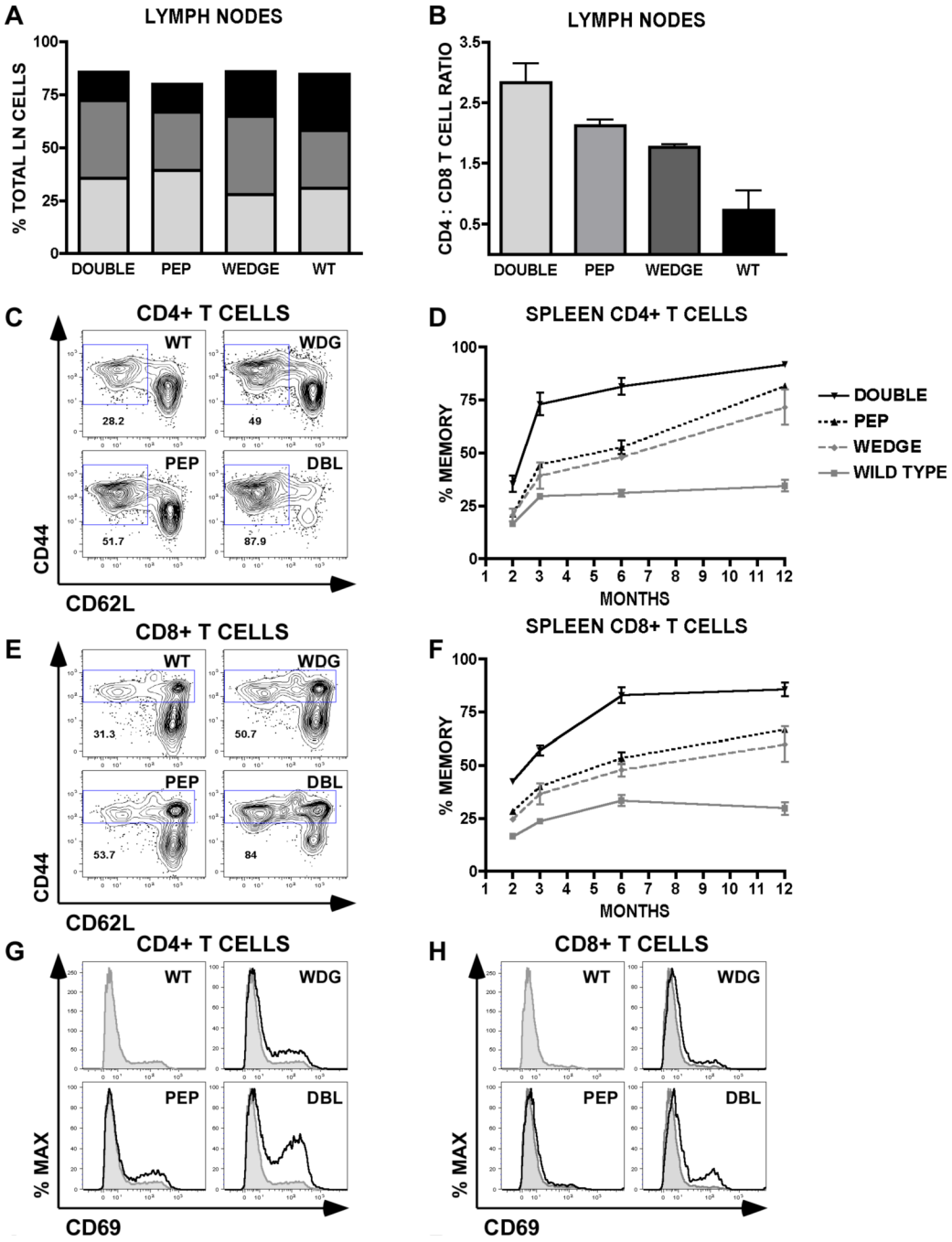

Figure 5.

T cell activation and differentiation in CD45$^{w/w}$/Pep$^{-/-}$ double mutant mice. (A) Lymph node composition at 6 months of age was determined by staining single cell suspensions with CD4 (dark gray), CD8 (black), and CD19 (light gray) mAb. (B) CD4 T cell / CD8 T cell ratios calculated from lymph node specimens at 6 months of age. Values are the mean of three biological replicates +/− SEM. (C) and (E) Representative cytometry plots of splenic CD4 and CD8 T cells stained with antibodies to CD62L and CD44 at 6 months of age. Gated fractions represent memory /effector cells. (D) and (F) Gated splenic T cell memory fractions depicted in (C) and (E) are plotted over time in (D) and (F) respectively. (G) and (H) Representative histograms of splenic CD4 T cells (G) and CD8 T cells (H) stained with CD69 to detect

activation status. Shaded histogram represents wild type for comparison. Animals were assessed at age 6 months. Data in all panels (A)–(G) are representative of at least 3 independent experiments performed at varying time points each involving 3 animals/genotype.

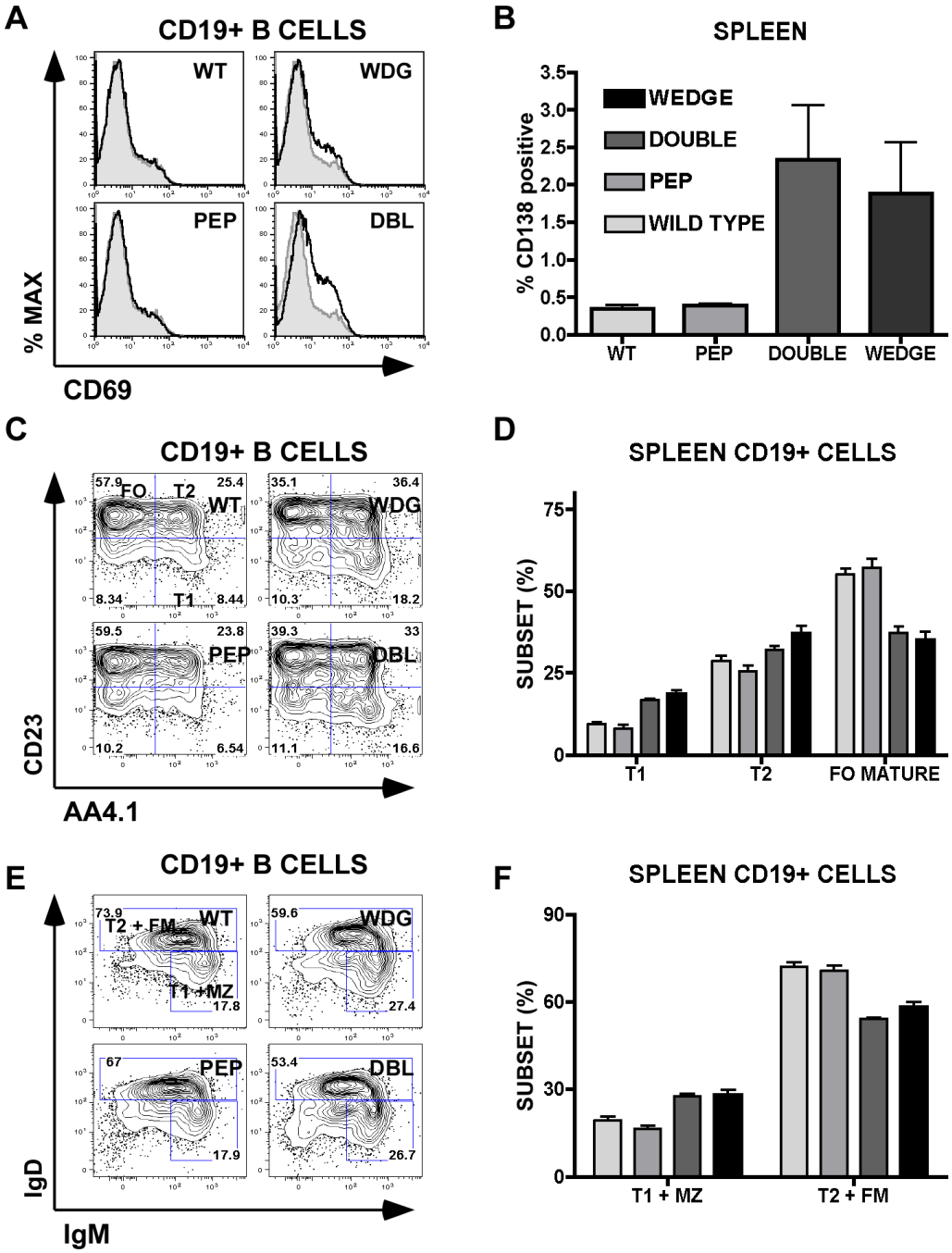

Figure 6.

Polyclonal B cell activation and perturbed B cell development in double mutant mice. (A) Representative histograms of lymph node CD19+ B cells stained with CD69 to detect activation status. Shaded histogram represents wild type for comparison. Animals were assessed at age 6 months. (B) Plasma cell marker CD138 expression among splenocytes (%) at age 3 months. (C) Representative cytometry plots of CD19+ splenocytes stained with CD23 and AA4.1 to identify transitional (T1, T2) and follicular mature (FO) B cell subsets. (D) Quantification of subsets identified in (C). (E) Representative cytometry plots of CD19+ splenocytes stained with IgM and IgD to identify transitional (T1, T2), marginal zone (MZ) and FO mature B cell subsets (FM). (F) Quantification of subsets identified in (E). Animals in figures (C)– (F) were

2 months of age at the time of analysis. In figures (B), (D), and (E) values are the mean of three biological replicates +/− SEM. All of the data presented are representative of at least 3 independent experiments at varying time points.

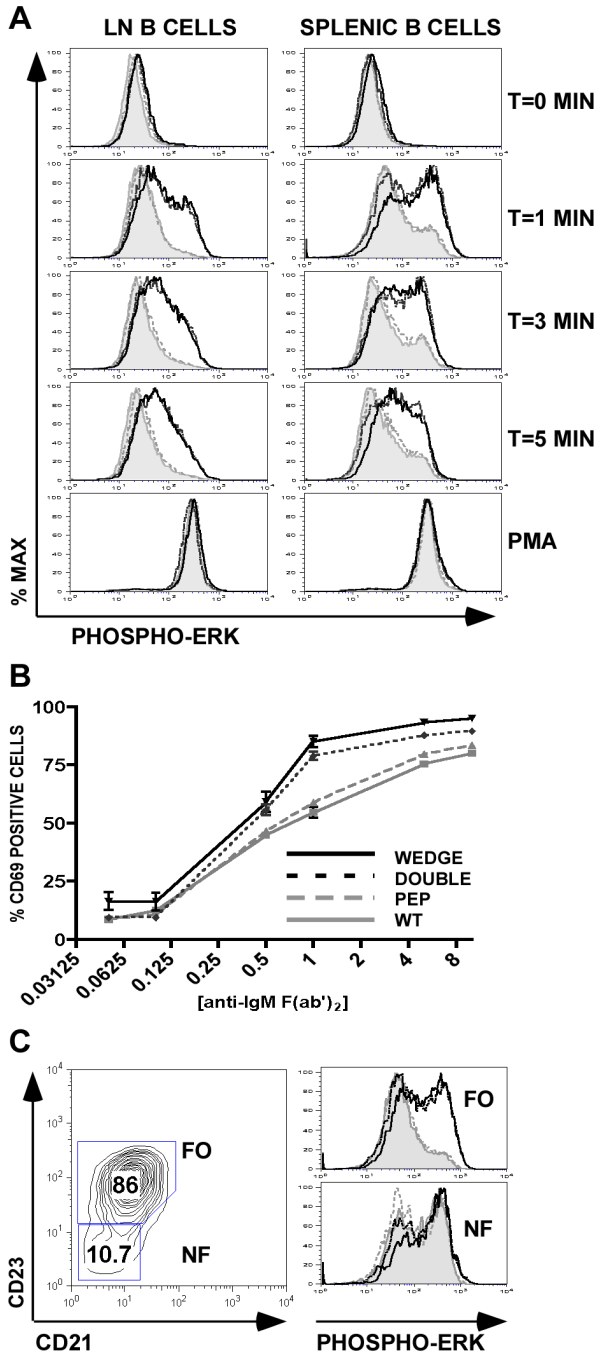

Figure 7.

Pep$^{-/-}$ does not contribute to CD45$^{W/W}$ B cell hyper-responsiveness. (A) Lymph node or splenic B cells were stimulated for varied periods of time (0, 1, 3 and 5 minutes) with goat anti-mouse IgM F(ab')$_2$ or, in the bottom panels, PMA. Fixed and methanol permeabilized cells were then stained with antibody against phospho-Erk and assessed by flow cytometry. Histograms represent gated B220+ B cells. Black solid line = CD45$^{w/w}$; Black dotted line = double mutant; Gray dashed line = Pep$^{-/-}$; Gray shaded histogram = WT. (B) Lymph node B cells were stimulated for 15 hours with goat anti-mouse IgM F(ab')$_2$ and stained for the activation marker CD69. The graph represents the percentage of total B cells upregulating CD69 at varied doses of stimulus. PMA reponses in all genotypes were identical. Values plotted

on $\log_2$ scale with each point representing mean +/− SEM of three biological replicates per genotype. Genotypes are identified as in (A). (C) Splenic B cells stimulated and stained as described in (A) were additionally stained with CD23 and CD21 to identify NF and FO cell populations as depicted in the lefthand panel. The upper histogram depicts FO B cell subsets while the lower histogram depicts NF B cell subsets. Genotypes are identified as in (A). All data presented in this figure are representative of at least 3 independent experiments.

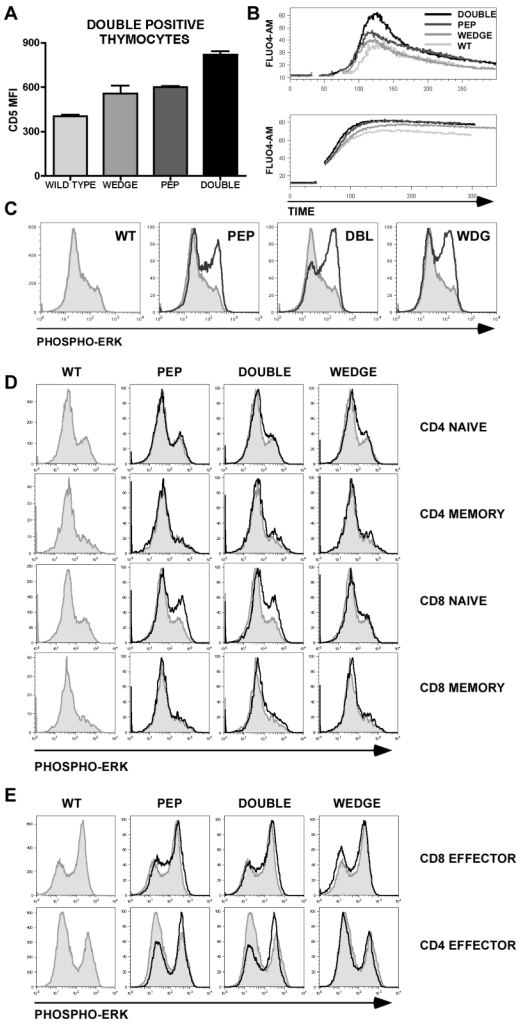

Figure 8.

Pep−/− and CD45 E613R alleles influence TCR signaling in a developmental stage-specific manner. (A) Graph depicts mean fluorescence intensity (MFI) for CD5 staining on gated double positive (DP) thymocytes. Values are the mean of three biological replicates +/− SEM and represent at least 5 independent experiments each involving 3 animals/genotype. (B) Intracellular calcium levels of Fluo-4 AM-loaded thymocytes (gated for small size to identify DP population). Green fluorescence was monitored by flow cytometry before and after stimulation with soluble anti-CD3ε antibody in the upper panel or ionomycin in the lower panel. Genotypes are identified as in Figure (A). Plots are representative of at least 4 independent experiments (C) DP thymocytes were stimulated with soluble anti-CD3ε. Fixed and methanol permeabilized cells were then stained with antibody against phospho-Erk and assessed by flow cytometry. Histograms represent gated DP thymocytes. Wild type DP thymocytes are represented by the shaded gray histogram in each plot for comparison. PMA responses in all genotypes were identical. Plots are representative of at least 5 independent experiments. (D) LN T cells were stimulated with anti-CD3 antibody, fixed and permeabilized with methanol and subsequently stained with antibodies to CD4, CD8, CD44, and phospho-Erk. Histograms represent staining for phospho-Erk on cells gated for CD4, CD8 and either CD44 low or high surface staining to identify naïve and memory subsets. Shaded histograms represent wild type for comparison. Plots are representative of at least three independent experiments each with three biological replicates /genotype. (E) In vitro generated effector

CD4 or CD8 T cells were stimulated, fixed, and permeabilized as described above, and subsequently stained with antibody to phospho-Erk. Histograms represent staining for phospho-Erk. Shaded histograms represent wild type for comparison. Plots are representative of two independent experiments.